

CXCR4 inhibitor AMD3100 disrupts the interaction of multiple myeloma cells with the bone marrow microenvironment and enhances their sensitivity to therapy

*Abdel Kareem Azab,^{1,2} *Judith M. Runnels,^{1,2} Costas Pitsillides,² Anne-Sophie Moreau,¹ Feda Azab,¹ Xavier Leleu,¹ Xiaoying Jia,¹ Renee Wright,³ Beatriz Ospina,³ Alicia L. Carlson,² Clemens Alt,² Nicholas Burwick,¹ Aldo M. Roccaro,¹ Hai T. Ngo,¹ Mena Farag,¹ Molly R. Melhem,¹ Antonio Sacco,¹ Nikhil C. Munshi,¹ Teru Hideshima,¹ Barrett J. Rollins,¹ Kenneth C. Anderson,¹ Andrew L. Kung,³ †Charles P. Lin,² and †Irene M. Ghobrial¹

¹Medical Oncology, Dana-Farber Cancer Institute and Harvard Medical School, Boston, MA; ²Advanced Microscopy Program, Center for Systems Biology and Wellman Center for Photomedicine, Massachusetts General Hospital, Boston; and ³Pediatric Oncology, Dana-Farber Cancer Institute, Children's Hospital Boston and Harvard Medical School, Boston, MA

The interaction of multiple myeloma (MM) cells with their microenvironment in the bone marrow (BM) provides a protective environment and resistance to therapeutic agents. We hypothesized that disruption of the interaction of MM cells with their BM milieu would lead to their sensitization to therapeutic agents such as bortezomib, melphalan, doxorubicin, and dexamethasone. We report that the CXCR4 inhibitor AMD3100 induces disruption of the interaction of MM cells with the

BM reflected by mobilization of MM cells into the circulation in vivo, with kinetics that differed from that of hematopoietic stem cells. AMD3100 enhanced sensitivity of MM cell to multiple therapeutic agents in vitro by disrupting adhesion of MM cells to bone marrow stromal cells (BMSCs). Moreover, AMD3100 increased mobilization of MM cells to the circulation in vivo, increased the ratio of apoptotic circulating MM cells, and enhanced the tumor reduction induced by bortezomib.

Mechanistically, AMD3100 significantly inhibited Akt phosphorylation and enhanced poly(ADP-ribose) polymerase (PARP) cleavage as a result of bortezomib, in the presence of BMSCs in coculture. These experiments provide a proof of concept for the use of agents that disrupt interaction with the microenvironment for enhancement of efficacy of cytotoxic agents in cancer therapy. (Blood. 2009;113:4341-4351)

Introduction

Multiple myeloma (MM) is the second most prevalent hematologic malignancy, and it remains incurable with a median survival of 3 to 5 years.^{1,2} Novel therapeutic agents, including bortezomib, thalidomide, and lenalidomide, and hematopoietic stem cell transplantation have led to a significant advancement in the treatment of patients with this disease.³⁻⁵ However, only 25% to 35% of patients respond to these agents in the relapsed setting,^{6,7} indicating that there is a need to improve the therapeutic activity of those agents.

The interaction of MM cells with extracellular matrix (ECM) proteins and bone marrow (BM) cells, as well as factors in the BM milieu (cytokines, chemokines, angiogenesis), plays a crucial role in MM pathogenesis and drug resistance.⁸⁻¹¹ The interactions of MM cells with the BM microenvironment activates proliferative and antiapoptotic signaling cascades.^{12,13} These molecular events are triggered either directly via cell adhesion molecule-mediated interactions of MM cells with BM stromal cells (BMSCs) and ECM or indirectly by growth factors released by BMSCs or MM cells or both.^{14,15} Current studies have focused on developing therapies that induce apoptosis of MM cells, even in the presence of the BM milieu, but even these have had limited success.¹⁶

MM is characterized by widespread involvement of the BM at diagnosis, implying (re)circulation into the peripheral blood (PB) and (re)entrance or homing of MM cells into new sites of the BM, a process termed trafficking.^{17,18} The selective homing of MM cells

to the BM depends on chemoattractants (chemokines) that regulate the process of homing and adhesion of MM cells to their specific microenvironment. Chemokines play a central role in lymphocyte trafficking and homing,¹⁹⁻²² specifically the chemokine stromal cell-derived factor-1 (SDF-1), and its receptor, CXCR4. SDF-1 induces modest proliferation of MM cells and induces phosphorylation of mitogen-activated protein kinase kinase 1/2 (MEK1/2), p42/44 mitogen-activated protein kinase (MAPK), and Akt in a time-dependent fashion in MM cell lines and primary MM cells.¹⁰ SDF-1 induces interleukin-6 (IL-6) and vascular endothelial growth factor (VEGF) secretion, indicating a role of SDF-1 in the support of MM growth.¹⁰ In addition, SDF-1 protects MM cells from dexamethasone-induced apoptosis,¹⁰ up-regulates very late activation antigen 4 (VLA4)-mediated cell adhesion to both fibronectin and vascular cell adhesion molecule-1 (VCAM-1),^{23,24} and increases invasion and matrix metalloproteinase (MMP) secretion in MM.^{24,25} Previous studies that used the CXCR4 inhibitor AMD3100 have shown that it induces significant mobilization of hematopoietic stem cells (HSCs) into the peripheral blood.²⁶ We previously showed that CXCR4 is critical for homing of MM cells to the bone marrow and that AMD3100 inhibits migration in vitro and homing in vivo, as well as downstream signaling through the phosphatidylinositol 3-kinase (PI3K)/Akt and extracellular signal-regulated kinase (ERK) signaling pathways.¹⁸ To date, there are no data on

Submitted October 29, 2008; accepted December 31, 2008. Prepublished online as *Blood* First Edition Paper, January 12, 2009; DOI 10.1182/blood-2008-10-186668.

*A.K.A. and J.M.R. contributed equally to this study.

†C.P.L. and I.M.G. are joint senior authors.

The online version of this article contains a data supplement.

The publication costs of this article were defrayed in part by page charge payment. Therefore, and solely to indicate this fact, this article is hereby marked "advertisement" in accordance with 18 USC section 1734.

© 2009 by The American Society of Hematology

whether MM cells can be mobilized into the circulation with the use of AMD3100 and whether these cells will be rendered more sensitive to therapeutic agents by disrupting their adhesion to the BM microenvironment. Targeting malignant cell trafficking would lead to new therapeutic approaches in MM and other malignancies, where it will alter the capacity of malignant cells to interact with their protective microenvironment by disrupting adhesion and inducing mobilization, leading to increased sensitivity to therapeutic agents. The use of the clinically available CXCR4 inhibitor, AMD3100, may be the first of a series of similar agents that induce sensitization by disruption of the interaction between MM cells and the BM microenvironment.

In this study, we test the hypothesis that disruption of the adhesion and homing of MM cells to the bone marrow niches induces sensitivity to apoptosis by therapeutic agents. The goals of this study were to test the effect of AMD3100 on (1) MM cell sensitivity to dexamethasone, melphalan, doxorubicin, and bortezomib *in vitro*; (2) the therapeutic effect of bortezomib on myeloma tumor regression *in vivo*; (3) mobilization of MM cells from established tumors to the circulation and the apoptotic effect of bortezomib *in vivo*; (4) MM cell adhesion and migration *in vitro* in response to AMD3100 and bortezomib; and (5) the effect of AMD3100 on the kinetics of mobilization of MM cells and HSCs *in vivo*.

Methods

In vitro studies

Cells, lentivirus infection, and reagents. Dexamethasone-sensitive human MM cell line MM.1S was kindly provided by Dr Steven Rosen (Northwestern University, Chicago, IL). The RPMI 8226 and OPM-2 human MM cell lines were purchased from ATCC (Manassas, VA). GFP-luciferin-Neo MM.1S cells were generated with the use of lentivirus infection as previously described.¹⁸

Primary MM cells were obtained from bone marrow samples from patients with the use of CD138⁺ microbead selection (Miltenyi Biotec, Auburn, CA). Similarly, HSCs were obtained from the bone marrows of the patients with MM with the use of CD34⁺ microbead selection. Informed consent was obtained from all patients in accordance with the Declaration of Helsinki. Approval of these studies was obtained by the Dana-Farber Cancer Institute Institutional Review Board. For the studies that used BMSCs, bone marrow aspirates were subjected to Ficoll-Paque gradient centrifugation (GE Healthcare, Little Chalfont, United Kingdom), and mononuclear cells (MNCs) were separated as in prior studies.²⁷ AMD3100, dexamethasone, and melphalan were obtained from Sigma-Aldrich (St Louis, MO), bortezomib was obtained from Millennium Pharmaceutical (Cambridge, MA), and SDF-1 was obtained from R&D Systems (Minneapolis, MN).

Detection of *in vitro* apoptosis. MM cells (MM.1S) were cultured with or without BMSCs. Nonadherent cells were discarded, and adherent cells were treated with bortezomib (0, 2.5, and 5 nM), dexamethasone (25 nM), melphalan (10 μ M), or doxorubicin (150 nM) in the presence or absence of AMD3100 (50 μ M) for 24 hours. Cells (10⁶) were then washed and resuspended in phosphate-buffered saline (PBS), annexin V-fluorescein isothiocyanate (FITC; 5 μ L/mL; Caltag Laboratories, Burlington, CA) and propidium iodide (PI; Invitrogen, Carlsbad, CA) were added and incubated for 20 minutes at 4°C. Cells were washed and analyzed for apoptosis with the use of flow cytometry as previously described.²⁸

Adhesion assays. We used an *in vitro* adhesion assay coated with fibronectin following the manufacturer recommendations (EMD Biosciences, San Diego, CA). Briefly, MM.1S (2 \times 10⁵) cells were incubated in the 96-well plate of adhesion with increasing concentrations of bortezomib (0, 2.5, and 5 nM) in the presence or absence of AMD3100 (50 μ M). After 2 hours at 37°C, nonadherent cells were washed from the wells, adherent cells were labeled with calcein-AM, and the intensity of fluorescence was measured at Ex/Em = 485/520 nm. The bovine serum

albumin (BSA)-coated well served as negative control, and poly-L-lysine-coated wells served as positive controls.

For the stromal cell adhesion assay, stromal cells were obtained as previously described,²⁷ and a confluent monolayer was generated by plating 10 \times 10⁵ BMSCs in a 96-well plate for 24 hours. MM.1S cells, prelabeled with calcein-AM, were treated with bortezomib or AMD3100 or both and plated in coculture with stromal cells for 2 hours at 37°C. Nonadherent cells were washed from the wells, and fluorescence intensity was assessed.

Transwell migration assay. Migration was determined by using the transwell migration assay (Corning Life Sciences, Acton, MA) according to the manufacturer's instructions and as previously described.²⁷ MM.1S cells incubated in 1% fetal bovine serum (FBS) were treated with increasing concentrations of bortezomib (0, 2.5, and 5 nM) with or without AMD3100 50 μ M for 90 minutes, and then placed in the migration upper chambers in the presence or absence of SDF-1 (30 nM) with 1% FBS in the lower chambers. After 4 hours of incubation, cells that migrated to the lower chambers were counted with the use of a Beckman Coulter cell counter (Fullerton, CA).

***In vitro* flow cytometric analyses of CXCR4 expression.** MM cells were treated for 6 and 24 hours with AMD3100, bortezomib 5 nM, or their combination, and CXCR4, VLA4, and intercellular adhesion molecule (ICAM) expressions were determined by flow cytometric analysis (Beckman Coulter) with the use of CXCR4-phycoerythrin (PE), VLA4-PE, and ICAM-PE and with immunoglobulin G (IgG)-PE isotype antibodies (BD Biosciences, San Jose, CA).

Immunoblotting. Immunoblotting was performed as previously described.²⁹ MM cells (MM.1S) were cultured with or without BMSC bortezomib (0, 2.5, and 5 nM) for 24 hours, in the presence or absence of AMD3100 (50 μ M). The following antibodies were used for immunoblotting: poly(ADP-ribose) polymerase (PARP), pAkt (Ser473), p-S6 ribosomal (Ser240/244; Cell Signaling Technology), and β -actin (Sigma-Aldrich).

Colony-forming assays. Colony-forming unit (CFU) assays were performed in the presence or absence of bortezomib (5 nM) or AMD3100 50 μ M or both in Iscove modified Dulbecco medium (IMDM) supplemented with 1% methylcellulose, 30% FBS, 1% BSA, 2 mM L-glutamine, plus recombinant human erythropoietin (3 U/mL), IL-3 (10 ng/mL), stem cell factor (50 ng/mL), and granulocyte-macrophage colony-stimulating factor (GM-CSF; 10 ng/mL). Semisolid cultures were performed in duplicates. Hematopoietic colonies were enumerated with an inverted microscope. Approximately 5 \times 10³ cells were cultured, and colonies (erythroid burst-forming units [BFU-Es], granulocyte-macrophage colony-forming units [CFU-GMs], macrophage colony-forming units [CFU-Ms], and granulocyte-macrophage-erythroid-megakaryocyte colony-forming units [CFU-GEMMs]) were counted at day 14.

In vivo studies

Animals. Approval of these studies was obtained by the Dana-Farber Cancer Institute and Massachusetts General Hospital Institutional Animal Care and Use Committees. Male, 7 to 9 weeks old, severe combined immunodeficient (SCID) mice were obtained from Charles River Laboratories (Wilmington, MA). Anesthesia was performed by intraperitoneal injections of ketamine (Bedford Laboratories, Bedford, OH) /xylazine (Lloyd Laboratories, Shenandoah, IA) at 80 mg/kg/12 mg/kg body weight (c). Mice subjected to multiple anesthetic treatments within a week were injected with 80 mg/kg/6 mg/kg ketamine/xylazine. Mice were killed by inhalation of CO₂.

MM animal model in SCID mice. Luc⁺/GFP⁺ MM.1S cells (2 \times 10⁶/mouse) were injected into the tail vein of 30 SCID mice. After 3 to 4 weeks, sufficient tumor progression occurred to be detected by bioluminescence imaging. Mice were randomly divided into 6 groups: group 1, control untreated mice; group 2, mice treated daily with 5 mg/kg AMD3100 subcutaneous injection; group 3, mice treated with intraperitoneal bortezomib injection of 0.25 mg/kg twice a week; group 4, mice treated with intraperitoneal bortezomib injection of 0.5 mg/kg twice a week; group 5, mice treated with intraperitoneal bortezomib injection of 0.25 mg/kg twice a week and daily with 5 mg/kg AMD3100 subcutaneous injection; and group 6, mice treated with intraperitoneal bortezomib injection of 0.5 mg/kg twice a week and daily with 5 mg/kg AMD3100 subcutaneous injection. Whole-body real-time bioluminescence imaging was performed as

previously described.^{30,31} Imaging was performed for estimation of tumor growth at 1, 3, 5, 9, 12, 15, 19, 22, 26, and 30 days after the beginning of the treatment. Moreover, mice were subjected to *in vivo* flow cytometry as described in "Detection of cell mobilization by *in vivo* flow cytometry" for detection of mobilization of tumor cells and apoptotic tumor cell in the circulation. BM niches in the mice were imaged by *in vivo* confocal microscopy.

Detection of tumor progression by bioluminescence imaging. Mice were injected with 75 mg/kg luciferin (Xenogen, Hopkinton, MA) and imaged for bioluminescence 10 minutes after the injection. The home-built bioluminescence system used an electron multiplying CCD (Andor Technology, Belfast, United Kingdom) with an exposure time of 15 seconds, an electron multiplication gain of 500-voltage gain \times 200, 5-by-5 binning, and background subtraction. Images were analyzed with the use of ImageJ software (National Institutes of Health, Bethesda, MD).

Mobilization of MM and HSCs. MM (CD138⁺) and HSCs (CD34⁺) cells were isolated from patients with MM as described in "Detection of cell mobilization by *in vivo* flow cytometry." For labeling, CD138⁺ and CD34⁺ pairs were incubated separately with DiO or DiD (Invitrogen) at a final concentration of 1 μ M in 0.1% BSA in RPMI 1640 for 30 minutes at 37°C in 5% CO₂ atmosphere. After labeling, cells were washed, and the 2 populations were mixed and resuspended in RPMI 1640 plus 2% FCS for coinjection into mouse tail vein at a concentration of 3×10^6 each/mouse. Mice were not manipulated for 3 days to allow complete homing of all cells, then mice were treated daily with 5 mg/kg AMD3100 subcutaneous injection, and mobilized cells were detected at days 1, 2, 3, and 4, by *in vivo* flow cytometry as described in "Detection of cell mobilization by *in vivo* flow cytometry."

Detection of cell mobilization by *in vivo* flow cytometry. *In vivo* flow cytometry is a new technology that allows real-time, continuous monitoring of fluorescent cells in the circulation of live animals without the need to draw blood samples.³² In these experiments, mice were anesthetized and placed on a heated stage (32°C), and an appropriate arteriole in the ear was chosen for obtaining measurements. The GFP and DiO fluorescence of circulating cells was excited by a 473-nm diode-pumped solid-state laser (Melles Griot, Carlsbad, CA) focused as a slit across the ear vessel. Signal was detected by a photomultiplier tube, through a 545/60-nm bandpass filter, and then digitized for analysis on a personal computer equipped with Matlab software (The MathWorks, Natick, MA). Likewise, fluorescence from DiD-labeled cells was excited with a 633-nm HeNe laser (JDS Uniphase, Milpitas, CA) and detected through a 670/40-nm filter.

Detection of apoptotic cells in the circulation by *in vivo* flow cytometry. Alexa Fluor 647-annexin (Invitrogen) was injected into the tail vein of the mice (5 μ g/mouse) immediately before *in vivo* flow cytometry. Quantification of green fluorescent protein-positive (GFP⁺; excitation, 442 nm) and annexin⁺ cells (excitation, 663 nm) were performed simultaneously with 2-color *in vivo* flow cytometry. The numbers of annexin⁺, GFP⁺, and annexin⁺/GFP⁺ cells were determined, and the ratio of apoptotic cells (annexin⁺ and annexin⁺/GFP⁺ cells) was compared with the total number of circulating cells and was calculated.

***In vivo* video rate confocal microscopy.** MM cell and vasculature of the BM niches in mice skull were imaged with *in vivo* confocal microscopy, as previously described.³³ A skin flap was made in the scalp of the mice to expose the underlying skull surface. Images of the tumors were captured in approximately 1-hour sessions. High-resolution images with cellular detail were obtained through the intact mouse skull at depths of up to 250 μ m from the surface of the skull with a 30 \times /0.9 NA water-immersion objective lens (Lomo, St Petersburg, Russia). Multiple imaging depths were acquired, and a maximum intensity z-projection was performed in ImageJ to merge the images. GFP was excited with a 491-nm solid-state laser (Dual Calypso; Cobolt AB, Stockholm, Sweden) and detected with a photomultiplier tube through a 528/19-nm bandpass filter (Semrock, Rochester, NY). Apoptotic cells were imaged by injection of annexin-Alexa Fluor 647, 1 hour before detection, which was excited with a 638-nm helium-neon laser (Radius; Coherent, Santa Clara, CA) and detected through a 680/25-nm bandpass filter (Chroma Technologies, Rockingham, VT). Blood vessels were imaged by injection of Angiosense 750 (VisEn Medical, Woburn, MA), which was excited with a 750-nm laser and captured through a 785/25-nm bandpass filter (Chroma Technologies). The frame rate of the confocal microscope was 30 frames/second. Images were captured, after averaging

30 frames, with a Macintosh computer (Apple, Cupertino, CA) equipped with an Active Silicon snapper card (Active Silicon, Chelmsford, MA)

Immunohistochemistry. Mice with MM tumors from the different treatment groups were dissected, and specimens from the femur, liver, and spleen were rinsed with PBS, fixed with 4% formaldehyde in PBS, dehydrated with ethanol, embedded in paraffin blocks, and sectioned. Sections from femur were stained for terminal uridine deoxynucleotidyl transferase dUTP nick-end labeling (TUNEL) for detecting DNA fragmentation that results from apoptotic signaling cascades in the cells in the bone marrow as previously described.³⁴ Sections from femur, liver, and spleen were stained with anti-human-CD138 antibodies (Ventana Stainer; Ventana Medical Systems, Tucson, AZ) for detection of tumor cells. Moreover, the numbers of CD138⁺ cells or TUNEL⁺ cells in 10 sections for each animal were counted, mean was calculated, and data were expressed as the percentage of control.

Statistical analysis

Results were reported as the mean plus or minus SD for experiments done in 3 replicates samples and were compared by the Student *t* test. Results were considered significantly different for *P* values less than .05.

Results

AMD3100 overcomes drug resistance induced by BMSCs in coculture with MM cell lines *in vitro*

To test our hypothesis that disruption of adhesion of MM cells to the BMSCs increases their sensitivity to cytotoxic agents such as bortezomib, we examined the effect of bortezomib on MM cell lines alone or in coculture with BMSCs in the presence or absence of AMD3100. We previously demonstrated that AMD3100 does not induce apoptosis in MM cells. Similarly, Figure 1A shows that AMD3100 does not induce an additional effect to bortezomib-induced apoptosis in MM.1S cells. However, in the presence of BMSCs, MM.1S showed resistance to apoptosis induced by bortezomib (Figure 1B), whereas treatment with AMD3100 restored sensitivity of MM.1S to bortezomib, which was reduced because of coculture with BMSCs (Figure 1B). The doses of AMD3100 and bortezomib used were obtained from previous studies and are achievable clinically. Similar results were obtained with other MM cell lines, including OPM-2 (Figure 1C) and RPMI 8226 (Figure 1D). To show that the effect of AMD3100 on MM cells is not specific to bortezomib, we tested the effect of AMD3100 on apoptosis of MM1.S cells when cocultured with BMSCs in the presence of other therapeutic agents, including dexamethasone, melphalan, and doxorubicin (Figure 1E). AMD3100 significantly enhanced apoptosis induced by these agents in the presence of BMSCs, similar to its effect in combination with bortezomib.

AMD3100 induces disruption of MM migration and adhesion to fibronectin and BMSCs

Investigation of the effect of AMD3100, bortezomib, and their combination on adhesion of MM cells showed that AMD3100 induced significant inhibition of adhesion to both fibronectin (Figure 2A) and BMSCs (Figure 2B). Similarly, bortezomib induced inhibition of MM adhesion in a dose-dependent manner; however, it had no additive effect when combined with AMD3100. The addition of IL-6 (25 ng/mL) or macrophage-inflammatory protein 1 α (MIP-1 α ; 100 pg/mL) did not alter the effect of AMD3100 or bortezomib on adhesion to fibronectin (data not shown). Moreover, AMD3100 and bortezomib did not affect the level of secretion of IL-6 or MIP-1 α by stromal cells or by the coculture of MM cells and stromal cells (data not shown). Similarly, in Figure 2C, we showed that AMD3100 and bortezomib significantly inhibited MM cell migration in response to SDF-1 α , compared with control untreated cells and showed an additive effect.

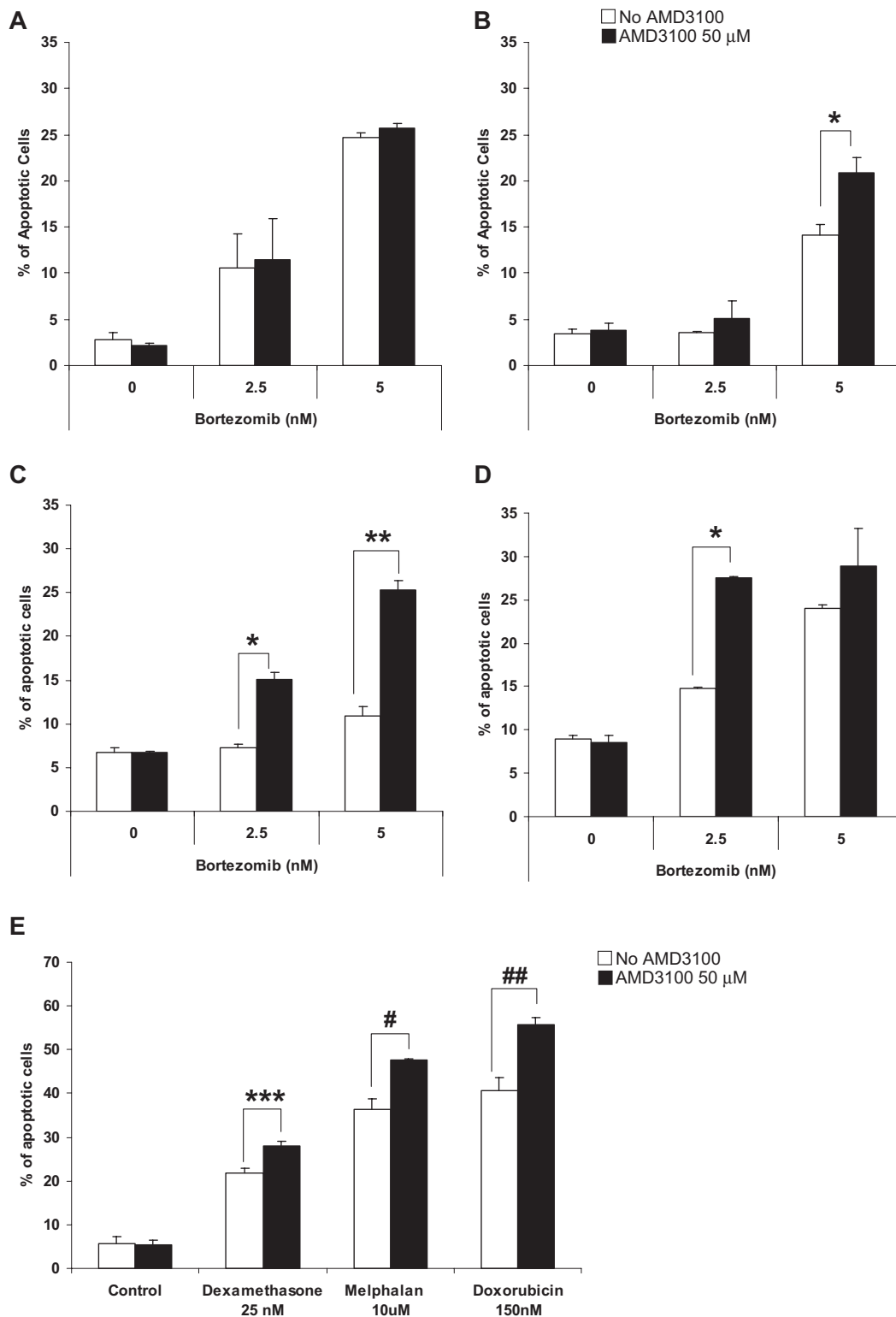


Figure 1. AMD3100 overcomes drug resistance to induction of apoptosis by therapeutic agents in MM cell lines induced by BMSCs in vitro. Apoptosis assay measured using Annexin staining by flow cytometry. (A) AMD3100 did not enhance the effect of bortezomib (2.5-5 nM) for 24 hours on MM.1S cells when those were cultured without BMSCs. However, treatment with AMD3100 (50 μ M) restored the sensitivity to bortezomib which was reduced as a result of coculture with BMSCs in the MM cell lines MM.1S (B), RPMI 8226 (C), and OPM-2 (D). Cells were treated with bortezomib either alone or in the presence of AMD3100 (50 μ M). This effect was not unique to bortezomib, but AMD3100 was shown to increase the sensitivity of MM.1S cells to treatment with dexamethasone 25 nM, melphalan 10 μ M, and doxorubicin 150 nM for 24 hours (E). * $P = .003$; ** $P < .001$; *** $P = .010$; # $P = .027$; ## $P = .048$. Error bars represent SD.

Effect of AMD3100 and bortezomib on CXCR4, VLA4, and ICAM

We tested whether the effects of AMD3100 and bortezomib in reducing MM cell adhesion and migration were due to changes in

cell-surface expression of CXCR4 or other adhesion molecules, which are highly expressed on the MM cells, with the use of flow cytometry. We found that AMD3100 (50 μ M) induced significant

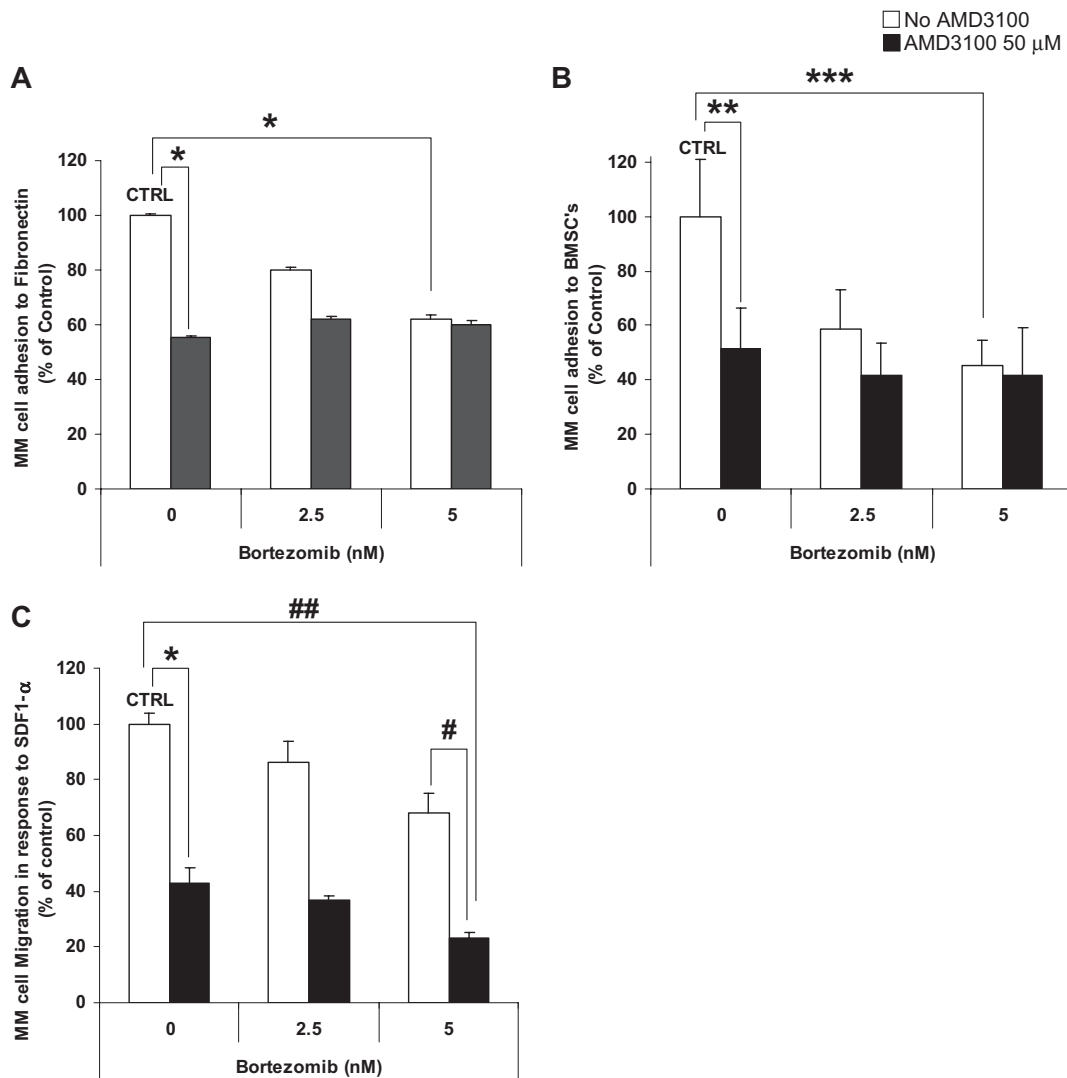


Figure 2. AMD3100 induces disruption of MM migration and adhesion to fibronectin and BMSCs. MM.1S cells pretreated for 2 hours with AMD3100 (50 μ M), bortezomib (2.5–5 nM), or their combination. MM.1S cells were used for adhesion to fibronectin (A), adhesion to BMSC (B), or migration (C) assays. AMD3100 induced 50% inhibition of adhesion to both fibronectin and BMSCs. Bortezomib induced a dose-dependent reduction of adhesion, when at concentration of 5 nM it induced 40% and 60% inhibition of adhesion to fibronectin and BMSCs, respectively, compared with control. The combination of AMD3100 and bortezomib did not show an additive effect compared with the effect of AMD3100 alone. In transwell migration assay of MM.1S cells to 30 nM SDF1, AMD3100 inhibited migration by greater than 60% of control. Bortezomib had a mild dose-dependent effect on migration of MM.1S cells, with 5 nM inhibiting migration by 20% compared with control. The combination of AMD3100 and bortezomib showed significant reduction of migration, specifically the combination of AMD3100 and 5 nM bortezomib showed 75% reduction of migration compared with control. * $P = .001$; ** $P = .015$; *** $P = .005$; # $P = .003$; ## $P < .001$. Error bars represent SD.

reduction of CXCR4 expression at 6 hours, but the expression of CXCR4 recovered at 24 hours. Similar results were observed in other MM cell lines (data not shown). Bortezomib had no effect on CXCR4 expression at 6 or 24 hours of treatment (5 nM; Figure 3A). The expression of the adhesion molecules ICAM and VLA4 did not change with either AMD3100 or bortezomib at 24 hours (Figure S1, available on the *Blood* website; see the Supplemental Materials link at the top of the online article).

AMD3100 restores PARP cleavage and inhibits Akt pathway activation induced by bortezomib

We further explored the signaling mechanism in which AMD3100 restores sensitivity to bortezomib. Figure 3B shows that AMD3100 alone does not affect PARP cleavage in MM cells when cultured with BMSCs. Bortezomib induced PARP cleavage in MM cells cocultured with BMSCs only at high doses (5 nM) but not at low

doses (2.5 nM). AMD3100 enhanced PARP cleavage induced by low doses of bortezomib in coculture with BMSCs, indicating that it can restore sensitivity of MM cells to low doses of bortezomib even in the presence of BMSCs.

In previous studies, we showed that bortezomib induces activation of pAkt, which could be a mechanism of resistance to apoptosis. Similarly, coculture of MM cells with BMSCs enhances the activity of pAkt in the MM cells,³⁵ whereas AMD3100 inhibits pAkt downstream of CXCR4.^{18,34} We, therefore, hypothesized that AMD3100 restores sensitivity to bortezomib-induced apoptosis through inhibition of signaling through the PI3K/Akt pathway. Figure 3B shows that bortezomib induced an increase of pAkt in MM.1S cells when cultured with BMSCs and that AMD3100 abolished the increase in phosphorylation of Akt and pS6, which is downstream of Akt, indicating a potential mechanism of synergy for apoptosis and inhibition of proliferation in the presence of AMD3100.

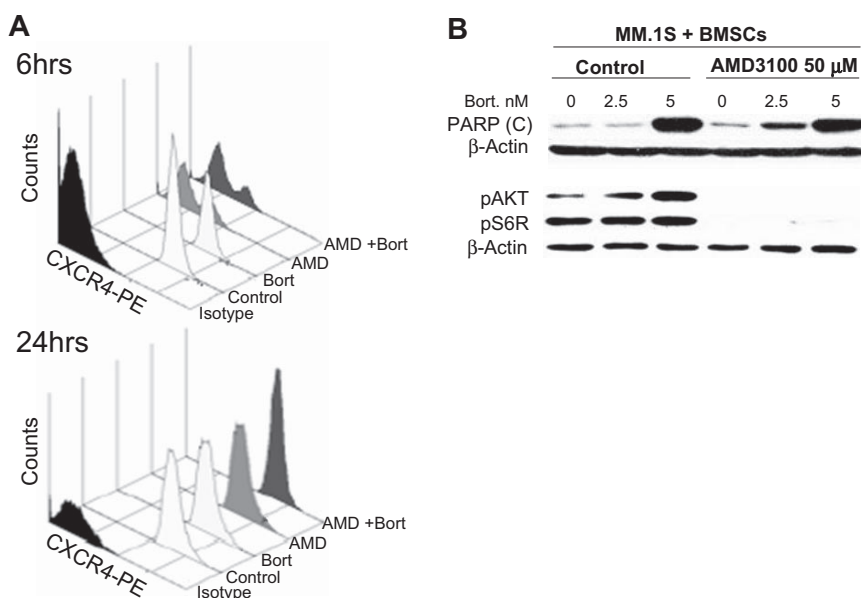


Figure 3. The effect of AMD3100 on PARP cleavage and phosphorylation of Akt in MM cells cocultured with BMSCs. (A) MM.1S cells treated with AMD3100 (50 μ M), bortezomib (5 nM), or their combination for 6 or 24 hours and expression of CXCR4 compared with nontreated cells were tested by flow cytometry. AMD3100 inhibited CXCR4 expression at 6 hours, but the expression recovered at 24 hours, whereas bortezomib had no effect on CXCR4 expression at either 6 or 24 hours. (B) MM.1S cells were cultured with BMSCs and treated with AMD3100 (50 μ M), bortezomib (0, 2.5, and 5 nM), or their combination overnight in PARP cleavage experiments or for 24 hours in pAkt and pS6R experiments. Immunoblotting with anti-PARP antibody showed that AMD3100 alone did not induce PARP cleavage in MM cells, but it increased the PARP cleavage induced by bortezomib especially at low doses. This shows that the increase of the apoptotic effect of bortezomib induced AMD3100. Moreover, immunoblotting for pAkt and pS6R showed that AMD3100 abolished the phosphorylation of Akt and S6R in MM cells in coculture with BMSCs, which was shown to be a resistance mechanism to bortezomib.

AMD3100 enhances tumor reduction induced by bortezomib in vivo

To test our hypothesis that disruption of adhesion of MM cells to the bone marrow niches increases their sensitivity to cytotoxic agents such as bortezomib, we examined the effect of AMD3100, bortezomib, or their combination on tumor progression in mice. Animals were treated with AMD3100 daily, bortezomib twice a week, or combination of both, and tumor progression was followed twice weekly with bioluminescence imaging of the mice. Mice treated with AMD3100 alone showed a similar pattern and rate of tumor growth compared with control mice. Mice treated with bortezomib showed a decrease in tumor burden in a dose-dependent manner; however, most importantly, the combination of AMD3100 and bortezomib showed a significant decrease in tumor burden compared with bortezomib alone (Figure 4A,B). Similar results were achieved with lower doses of bortezomib when combined with AMD3100 daily treatment (Figure S2).

We further confirmed that tumor reduction was associated with induction of apoptosis in MM cells in the bone marrow with TUNEL assay. As shown in Figure 4C and D, there was no difference in the number of apoptotic cells between the control and the AMD3100-treated groups, whereas treatment with bortezomib increased the number of apoptotic cells in the bone marrow, and the combination of AMD3100 and bortezomib induced a further increase in the number of apoptotic cells compared with treatment with bortezomib alone.

To test the pattern of tumor involvement of different organs of the tested groups, we used immunohistochemistry for human CD138⁺ to detect tumor cells. The AMD3100-treated group was similar to that of the control group in the BM and in liver and spleen, indicating that mobilization of MM cells by AMD3100 does not lead to engraftment of MM cells into extramedullary sites (Figure 4C). However, there was a significant decrease of tumor cells present in BM, liver, and spleen in the bortezomib-treated group, and a significant decrease was obtained in the group treated with combination of AMD3100 and bortezomib.

AMD3100 mobilizes MM cell to the circulation and sensitizes them to bortezomib-induced apoptosis in vivo

We then investigated the in vivo mechanism by which AMD3100 enhances tumor reduction induced by bortezomib. Our hypothesis was that disruption of adhesion of MM cells to BM microenvironment cells and milieu leads to increased sensitivity to bortezomib. We used the number of mobilized cells in the circulation as a surrogate measurement of disruption of adhesion in vivo.

We obtained the data correlating the amount of viable circulating cells (by in vivo flow cytometry) with tumor burden in the bone marrow (by bioluminescence) in the different treatment groups (Figure 5A) and found that the number of circulating cells was in linear correlation with the tumor burden. However, the extent of correlation, in which we compared the number of circulating cells at the same tumor burden, expressed by the slope of the linear correlation, varied between the different treatment groups. Figure 5B shows that the slope in the AMD3100-treated group was approximately double of that in the control group, indicating that more cells were mobilized to the circulation by AMD3100. Bortezomib did not show a significant decrease compared with the control group. However, the combination of bortezomib and AMD3100 reduces significantly the number of circulating cells compared with AMD3100 alone. This indicates that MM cells showed high sensitivity to bortezomib in the circulation.

Furthermore, we directly detected the number of apoptotic MM cells in the circulation of mice with annexin staining of apoptotic cells in real-time monitoring of in vivo flow cytometry and in vivo confocal microscopy imaging of the bone marrow niches. Figure 5C shows that the number of apoptotic circulating cells increased in response to bortezomib treatment in a dose-dependent manner, and treatment with AMD3100 alone did not significantly increase the ratio of apoptotic cells. However, the combination of AMD3100 and bortezomib significantly increased the ratio of apoptotic circulating cells compared with the control and bortezomib-treated groups. In vivo confocal imaging confirmed that the apoptotic MM cells were found in the vasculature of the bortezomib and AMD3100 group but not in the control group (Figure 5D).

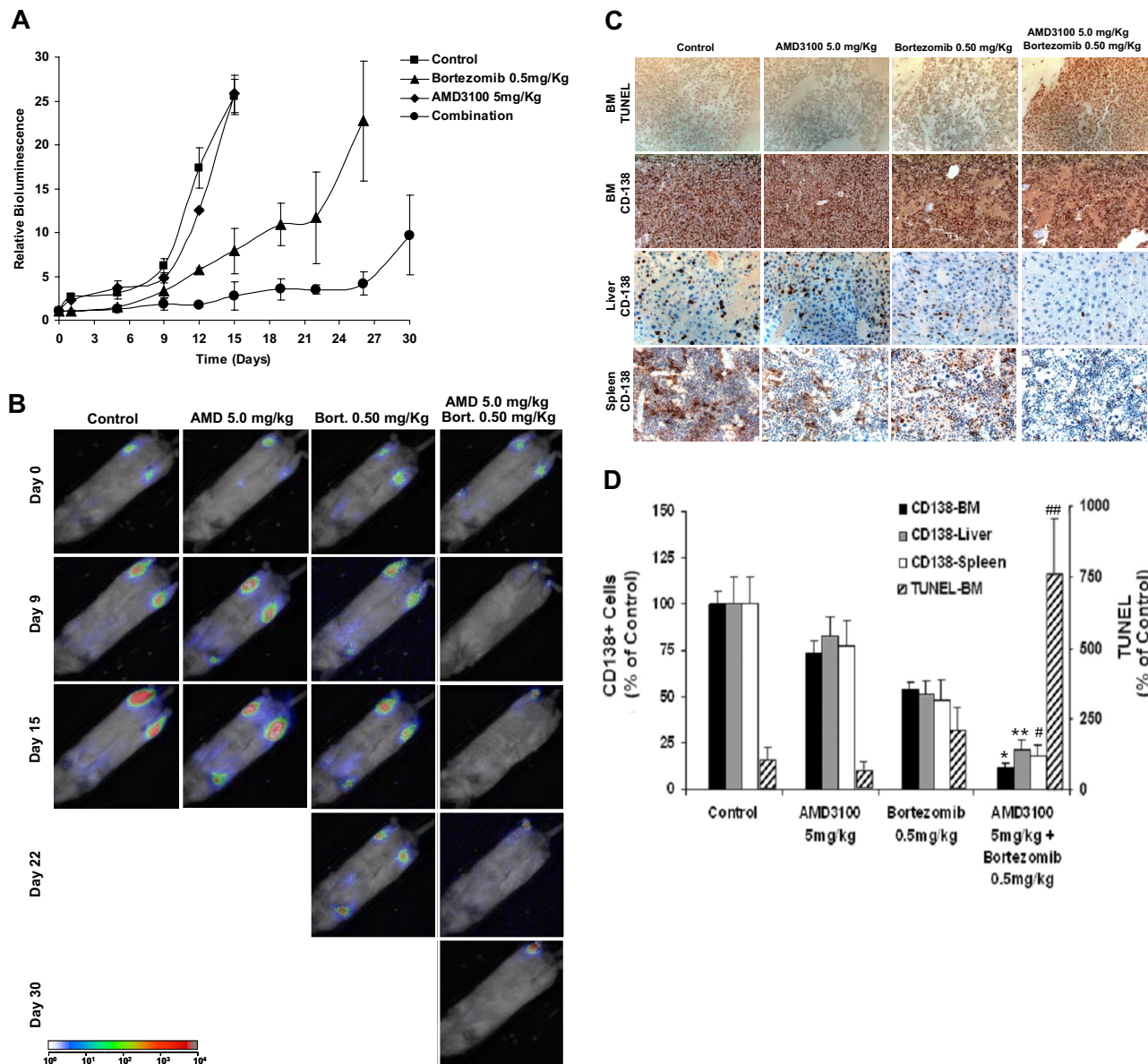


Figure 4. AMD3100 enhances tumor reduction induced by bortezomib in vivo. Mice were treated with AMD3100 (5 mg/kg, daily), bortezomib (0.5 mg/mL, twice weekly), or their combination and were compared with the control untreated group (A). Tumor growth was determined by bioluminescence imaging. Tumor growth in the AMD3100-treated group was similar to the control group, whereas the bortezomib-treated group showed reduction in tumor progression compared with control ($P = .041$), and the mice treated with the combination of AMD3100 and bortezomib showed significant tumor reduction compared with control ($P = .001$) and bortezomib alone ($P = .021$). Each data point represents 3 to 5 mice. Error bars represent SD. (B) Representative bioluminescence images of each treatment group with time. (C) Immunohistochemistry of specimens taken from BM, liver, and spleen. Top panel shows induction of apoptosis of MM cells in the BM detected by TUNEL assay. AMD3100 did not induce apoptosis compared with control, whereas the bortezomib-treated group showed low levels of apoptosis in the BM, and the combination of AMD3100 and bortezomib showed significant induction of apoptosis. The bottom 3 panels represent tumor spread in the BM, liver, and spleen by staining with anti-human CD138, showing that AMD3100 had a minimal effect on reducing the number of plasma cells present in the BM, liver, and spleen. However, bortezomib and more significantly the combination of bortezomib and AMD3100 showed reduction of tumor burden in the BM, liver, and spleen. Images were taken at 40 \times magnification with Leica DMLB microscope. (D) Quantification of the number of CD138 $^{+}$ cells in the BM, liver, and spleen and of TUNEL $^{+}$ cells in the BM. Statistically significant differences were found between numbers of CD138 $^{+}$ and TUNEL $^{+}$ cells in the bortezomib-treated group and the bortezomib + AMD3100-treated group. * $P < .001$; ** $P = .002$; # $P = .021$; ## $P < .016$. Error bars represent SD.

AMD3100 induces mobilization of MM cells with different kinetics compared with HSCs in vivo

We first investigated whether the kinetics of trafficking of MM cell lines would reflect accurately those of primary patient samples. We therefore studied homing of MM.1S cells compared with primary CD138 $^{+}$ MM cells. The kinetics of homing were similar between MM.1S and primary MM cells with rapid exit of the cells out of the circulation within 1 hour after tail vein injection (data not shown); this was in accord with our previous studies of homing of MM cells.¹⁸

We then investigated whether AMD3100 induces mobilization of MM cells in vivo and whether the kinetics of mobilization of malignant cells differed from that of HSCs. For these experiments, we used MM.1S cells, primary MM (CD138 $^{+}$) cells, and HSCs (CD34 $^{+}$) from the patients with MM. The mobilization studies were performed 3 days after cell injection to allow complete homing of the cells into the bone marrow niches. We then monitored daily mobilization of MM.1S cell line, primary MM cells, and primary HSCs in response to multiple daily treatments with AMD3100. Figure 6A shows that both the MM.1S cell line

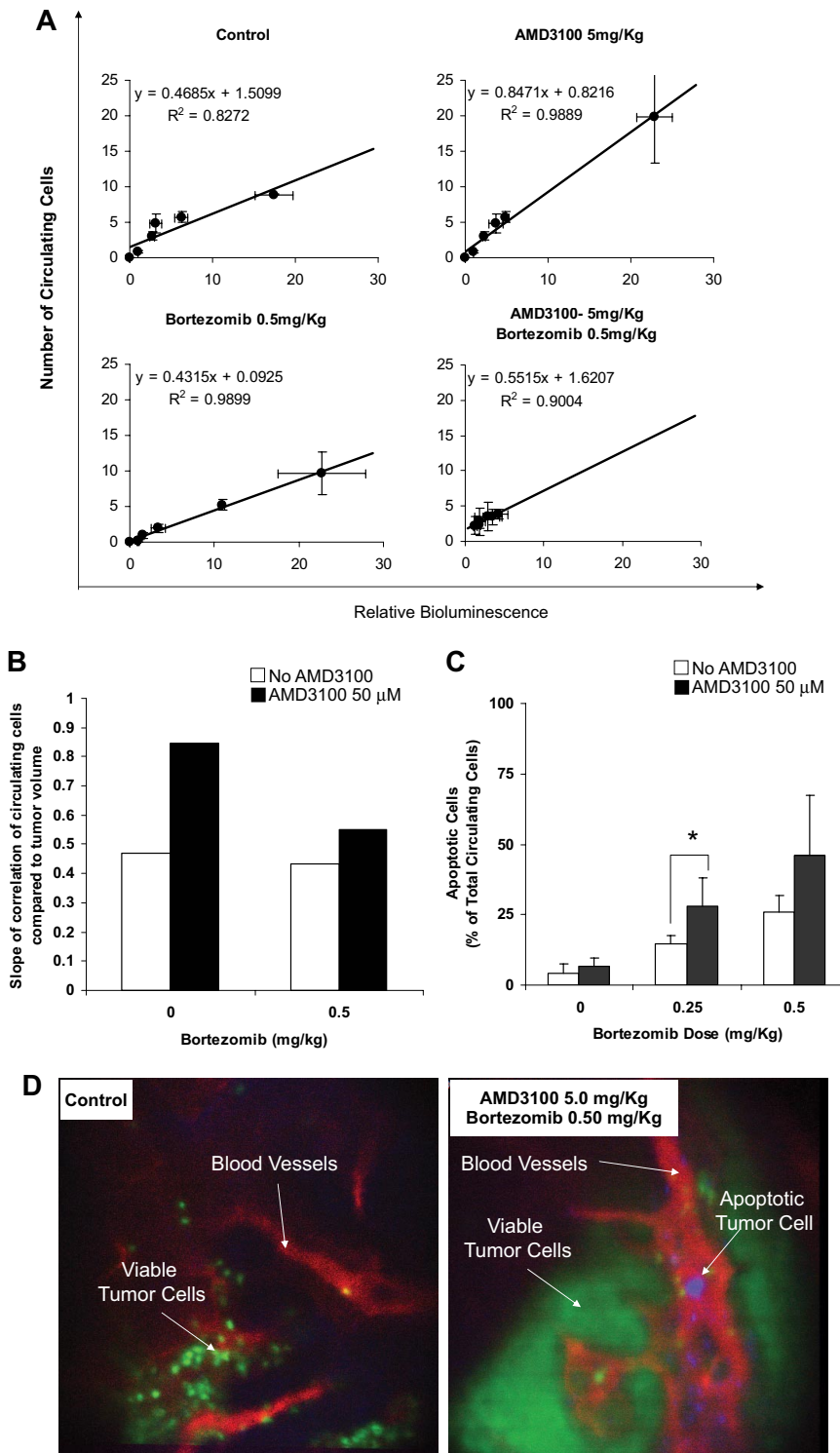


Figure 5. AMD3100 mobilizes MM cells to the circulation and sensitizes them to bortezomib-induced apoptosis in vivo. (A) Correlation of the number of viable circulating cells with tumor burden in the bone marrow. The number of circulating cells was in direct linear correlation with the tumor burden. Error bars represent SD. (B) Comparison of the slope of the linear correlations, which represents the amount of the mobilized MM cells per 1 unit of tumor burden. AMD3100 showed intensive mobilization of MM cells. Bortezomib did not show a significant decrease compared with the control group. However, the combination of bortezomib and AMD3100 reduces significantly the number of circulating cells compared with AMD3100 alone. (C) The ratio of apoptotic/total MM cells in the circulation detected by in vivo real-time flow cytometry. AMD3100 did not induce apoptosis compared with the control. Bortezomib showed a dose-dependent induction of apoptosis, which was enhanced by daily treatment with AMD3100. Error bars represent SD. (D) Representative in vivo confocal images of BM niches of control and combination of AMD3100 and bortezomib-treated mice, showing viable MM cells (green), apoptotic MM cells (violet), and blood vessels (red). These images show that apoptotic MM cells were present in the circulation of mice treated with the combination of AMD3100 and bortezomib and absent in the control mice. * $P = .046$.

and the MM primary cells showed continuous increase in the number of mobilized cells during the first 2 days of treatment and reached a plateau after the third day of treatment. In contrast, the number of circulating HSCs was higher in the first 2 days and decreased by the third day. On the basis of these kinetic differences, bortezomib treatment of established tumor experiments was started 3 days after the beginning of AMD3100 treatment. To further investigate whether AMD3100 or bortezomib induced cytotoxicity in HSCs, we performed colony formation assays with AMD3100, bortezomib, or their combination. As shown in Figure 6B, neither

AMD3100 nor bortezomib nor their combination had cytotoxic activity on colony-forming units of HSCs progenitors.

Discussion

MM represents a malignancy that specifically homes to the bone marrow, which provides a protective niche from therapeutic agents.³⁶ Recent advances in the treatment of MM with novel

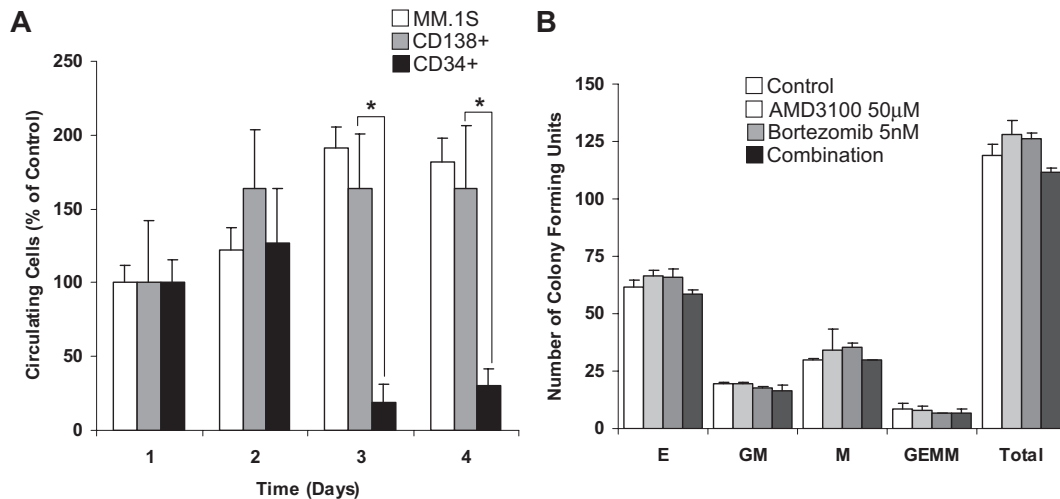


Figure 6. AMD3100 mobilizes MM cells and CD34⁺ HSCs in different kinetics and does not induce cytotoxicity of hematopoietic progenitor cells. (A) Mobilization of MM.1S, MM patient sample CD138⁺, and MM patient sample CD34⁺ cells after daily treatment of AMD3100 (5 mg/kg) detected by in vivo flow cytometry. AMD3100 induced similar and continuous mobilization of MM.1S and patient sample CD138⁺ cells at days 2, 3, and 4, whereas CD34 mobilization occurred on day 1 and decreased at days 2 and 3. (B) Colony-forming assays show that treatment with AMD3100 (50 μM), bortezomib (5 nM), or their combination had no significant cytotoxic effect on colony-forming units of erythroid (E), granulocyte-macrophage (GM), macrophage (M), and granulocyte-erythrocyte-monocyte-megakaryocyte (GEMM) origin. **P* = .002. Error bars represent SD.

therapeutic agents such as thalidomide, bortezomib, and lenalidomide that target the MM cells as well as the bone marrow microenvironment have induced significant responses.⁷ However, many patients do not respond to these agents, indicating that further advances are required.⁷ In this study, we propose a novel concept of therapy, in which disruption of the interaction of malignant cells with their protective environment by AMD3100 will sensitize them to cytotoxic therapy. These experiments are a proof of concept for implementation of the same approach in other hematologic malignancies and solid tumor metastasis.

We first demonstrated that the CXCR4 inhibitor AMD3100 sensitized MM cells to overcome resistance to therapy induced by BMSCs in vitro. This concept was not limited to bortezomib therapy alone but also occurred with other agents, including dexamethasone, melphalan, and doxorubicin. We then used a new mouse model with the use of GFP⁺ luciferase⁺ MM cells that enabled us to investigate the effect of AMD3100, bortezomib, and their combination on tumor progression with bioluminescence imaging, as well as in vivo flow cytometry, to measure the number of circulating MM cells and in vivo induction of apoptosis. We showed that AMD3100 does not induce a more aggressive behavior of the MM cells, and there was neither an increase in tumor progression nor an engraftment of MM in extramedullary sites in the AMD3100-treated mice compared with control mice. Most importantly, we showed that AMD3100 significantly enhanced the effect of bortezomib on tumor regression in the BM and distant organs.

To determine the mechanisms by which AMD3100 enhances the sensitivity of MM cells to bortezomib and other therapeutic agents when cocultured with stromal cells, we first examined the effect of these 2 agents on adhesion and migration of MM cells. We showed that both AMD3100 and bortezomib inhibited adhesion to fibronectin and BMSCs, indicating that disruption of adhesion is not the only mechanism by which AMD3100 enhances the effect of bortezomib. Other agents such as dexamethasone, doxorubicin, and melphalan do not inhibit adhesion to stromal cells; therefore, their in vivo activity maybe further enhanced by AMD3100. We then showed that AMD3100 reduces migration of MM cells in response to SDF in an additive effect with bortezomib, potentially indicating that AMD3100 prevents MM cells from migrating to BM niches

with high levels of SDF-1 (such as the osteoblastic niches), and by doing so induces sensitivity to bortezomib. We then examined the effect of AMD3100 on surface expression of CXCR4 and adhesion molecules highly expressed on MM cells, such as VLA4 and ICAM, and found no significant effect of these agents on the expression of adhesion molecules. AMD3100 inhibited CXCR4 expression at early time points, but the effect was reversible at 24 hours. There was no effect of AMD3100 or bortezomib on the surface expression of VLA4 or ICAM, indicating that the effect of AMD3100 is not through modulation of surface expression of adhesion molecules. On the basis of this, we then examined the effect of these agents on intracellular signaling pathways. We specifically focused on the Akt signaling pathway. Previous studies have shown that Akt is activated in response to adhesion of MM cells with BMSCs³⁷ and that bortezomib enhances Akt phosphorylation. CXCR4 is known to regulate the PI3K/Akt pathway. We, therefore, hypothesized that AMD3100 enhances activity of bortezomib by inhibiting Akt phosphorylation and therefore abolishes resistance induced by this pathway in response to adhesion to stromal cells.

To test the effect of mobilization of MM cells from the BM to the circulation, we tested the amount of circulating cells (detected by in vivo flow cytometry) in the different treatment groups at different time points compared with the tumor burden (detected by bioluminescence). We found a direct linear correlation between the tumor burden and the number of circulating cells with high coefficient of determination (R^2) in all the groups. The slope of linear correlation represents the number of cells detected in the circulation per 1 unit of tumor burden detected by bioluminescence. In the group treated with AMD3100, the slope of correlation was 1.8 times higher than the slope of correlation in the control group, representing a significant increase in mobilization of MM cell from the BM to the circulation compared with the control group. However, in the group treated with bortezomib and AMD3100, the slope was similar to that of the control group and the group treated with bortezomib alone, indicating that the cells that were mobilized to the circulation with AMD3100 were killed by bortezomib. We further confirmed these results by direct detection of MM apoptotic cells in the circulation by in vivo flow cytometry and confocal microscopy and showed that treatment

with AMD3100 alone did not induce apoptosis, bortezomib induced apoptosis in a dose-dependent manner, and the combination of AMD3100 and bortezomib significantly increased the ratio of apoptotic circulating cells compared with the control and bortezomib-treated groups with the use of *in vivo* flow cytometry.

AMD3100 has been tested in several clinical trials for HSC mobilization and showed significant improvement in the number of CD34⁺ cells mobilized, even in patients who failed to mobilize with granulocyte CSF (G-CSF).¹³ The mobilization peak of HSCs in healthy volunteers occurred during the first day after intravenous injection of AMD3100.³⁸ A phase 1 clinical trial using AMD3100 in combination with G-CSF for mobilization of HSCs in patients with MM and lymphoma resulted in a rapid and significant increase in the CD34⁺ counts at 4 and 6 hours after a single injection of the drug.^{26,39,40} No late sequelae of AMD3100 administration were noted.³⁹ Engraftment of AMD3100-mobilized cells was prompt; however, the previous studies did not evaluate the mobilization of malignant cells in conjunction with HSCs.²⁶ Although it was reported that G-CSF induces mobilization of HSCs and may potentially also induce mobilization of malignant cells, we chose to use AMD3100 because it has shown higher efficacy in the degree of mobilization of HSCs compared with G-CSF in previous clinical trials.³⁸ We investigated the kinetics of MM mobilization compared with that of HSCs mobilization, as expressed by the number of circulating cells, and showed that AMD3100 induces mobilization of malignant cells as a surrogate marker of disruption of adhesion. The kinetics of mobilization of MM cells were different from the HSCs; MM cells showed consistent mobilization after 3 days of daily injection of AMD3100 compared with a maximum at day 2 for HSCs. These differences in kinetics were exploited to determine the best timing of bortezomib injection after AMD3100 to minimize toxicity on mobilized HSCs. The mechanisms by which AMD3100 induces different mobilization kinetics in MM cells and HSCs is beyond the scope of this study and will be further explored in future studies. However, we hypothesize that it is related to intrinsic differences in CXCR4 activity or expression in MM cells compared with HSCs. We further confirmed that neither AMD3100 nor bortezomib nor their combination had cytotoxic effects on HSCs with the colony formation test, indicating that the use of these drugs should not induce significant cytopenias in future clinical trials.

In summary, our data show that AMD3100 disrupts the interaction of MM cells to the BM *in vitro* and *in vivo*, leading to

enhanced sensitivity to bortezomib. This concept may lead to novel approaches in MM therapy, by modulating the capacity of malignant cells to reside in their microenvironment. These studies may also be applied to other hematologic malignancies and to metastasis in solid tumors. Other novel therapeutic agents available in clinical trials that can be used for disrupting homing of MM cells include other CXCR4 inhibitors in clinical development or inhibitors of other chemokine receptors and adhesion receptors. In addition, agents that target trafficking can be used in low doses as maintenance therapies after cytoreduction with conventional therapies to prevent/delay progression of disease in minimal residual disease states by disrupting the trafficking of MM cells in and out of the BM. These trials may significantly enhance responses and overcome resistance in the treatment of MM and other malignancies.

Acknowledgments

This work was supported in part by R01CA125690, National Institutes of Health (NIH, Bethesda, MD) EB000664, the Leukemia & Lymphoma Society (White Plains, NY), and Multiple Myeloma Research Foundation (MMRF, Nowalk, CT).

Authorship

Contribution: A.K.A., J.M.R., C.P., A-S.M., F.A., X.L., X.J., R.W., B.O., A.L.C., and C.A. performed the research; A.K.A., J.M.R., F.A., N.B., A.M.R., H.T.N., M.F., M.R.M., A.S., N.C.M., T.H., B.J.R., K.C.A., A.L.K., C.P.L., and I.M.G. analyzed the data; A.K.A., J.M.R., C.P.L., and I.M.G. designed the study; and A.K.A. and I.M.G. wrote the paper.

Conflict-of-interest disclosure: I.M.G. and K.C.A. are on speakers bureaus for Millennium, Celgene, and Novartis. K.C.A. is an advisor for Celgene and Millenium. B.J.R. is an advisor for ProtAffin Biotechnologie AG. The remaining authors declare no competing financial interests.

Correspondence: Charles P. Lin, Wellman Center for Photomedicine and Center for Systems Biology, Massachusetts General Hospital, Boston, MA 02114; e-mail: lin@helix.mgh.harvard.edu; and Irene M. Ghobrial, Medical Oncology, Dana-Farber Cancer Institute, 44 Binney St, Mayer 548A, Boston, MA 02115; e-mail: Irene_ghobrial@dfci.harvard.edu.

References

- Kyle RA, Rajkumar SV. Multiple myeloma. *N Engl J Med*. 2004;351:1860-1873.
- Jemal A, Murray T, Ward E, et al. Cancer statistics, 2005. *CA Cancer J Clin*. 2005;55:10-30.
- Richardson PG. A review of the proteasome inhibitor bortezomib in multiple myeloma. *Expert Opin Pharmacother*. 2004;5:1321-1331.
- Richardson PG, Mitsiades CS, Hideshima T, Anderson KC. Novel biological therapies for the treatment of multiple myeloma. *Best Pract Res Clin Haematol*. 2005;18:619-634.
- Harousseau JL. Stem cell transplantation in multiple myeloma (0, 1, or 2). *Curr Opin Oncol*. 2005;17:93-98.
- Richardson PG, Barlogie B, Berenson J, et al. A phase 2 study of bortezomib in relapsed, refractory multiple myeloma. *N Engl J Med*. 2003;348:2609-2617.
- Ghobrial IM, Leleu X, Hatjiharissi E, et al. Emerging drugs in multiple myeloma. *Expert Opin Emerg Drugs*. 2007;12:155-163.
- Pagnucco G, Cardinale G, Gervasi F. Targeting multiple myeloma cells and their bone marrow microenvironment. *Ann N Y Acad Sci*. 2004;1028:390-399.
- Damiano JS, Cress AE, Hazlehurst LA, Shtil AA, Dalton WS. Cell adhesion mediated drug resistance (CAM-DR): role of integrins and resistance to apoptosis in human myeloma cell lines. *Blood*. 1999;93:1658-1667.
- Hideshima T, Chauhan D, Hayashi T, et al. The biological sequelae of stromal cell-derived factor-1alpha in multiple myeloma. *Mol Cancer Ther*. 2002;1:539-544.
- Damiano JS, Dalton WS. Integrin-mediated drug resistance in multiple myeloma. *Leuk Lymphoma*. 2000;38:71-81.
- Hideshima T, Nakamura N, Chauhan D, Anderson KC. Biologic sequelae of interleukin-6 induced PI3-K/Akt signaling in multiple myeloma. *Oncogene*. 2001;20:5991-6000.
- Hideshima T, Podar K, Chauhan D, Anderson KC. Cytokines and signal transduction. *Best Pract Res Clin Haematol*. 2005;18:509-524.
- Gupta D, Treon SP, Shima Y, et al. Adherence of multiple myeloma cells to bone marrow stromal cells upregulates vascular endothelial growth factor secretion: therapeutic applications. *Leukemia*. 2001;15:1950-1961.
- Akiyama M, Hideshima T, Hayashi T, et al. Cytokines modulate telomerase activity in a human multiple myeloma cell line. *Cancer Res*. 2002;62:3876-3882.
- Hideshima T, Akiyama M, Hayashi T, et al. Targeting p38 MAPK inhibits multiple myeloma cell growth in the bone marrow milieu. *Blood*. 2003;101:703-705.
- Lapidot T, Dar A, Kollet O. How do stem cells find their way home? *Blood*. 2005;106:1901-1910.
- Alsayed Y, Ngo H, Runnels J, et al. Mechanisms of regulation of CXCR4/SDF-1 (CXCL12)-dependent migration and homing in multiple myeloma. *Blood*. 2007;109:2708-2717.

19. Kucia M, Reca R, Miekus K, et al. Trafficking of normal stem cells and metastasis of cancer stem cells involve similar mechanisms: pivotal role of the SDF-1-CXCR4 axis. *Stem Cells*. 2005;23:879-894.
20. Li S, Huang S, Peng SB. Overexpression of G protein-coupled receptors in cancer cells: involvement in tumor progression. *Int J Oncol*. 2005;27:1329-1339.
21. Lopez-Giral S, Quintana NE, Cabrerizo M, et al. Chemokine receptors that mediate B cell homing to secondary lymphoid tissues are highly expressed in B cell chronic lymphocytic leukemia and non-Hodgkin lymphomas with widespread nodular dissemination. *J Leukoc Biol*. 2004;76:462-471.
22. Nakayama T, Hieshima K, Izawa D, Tatsumi Y, Kanamaru A, Yoshie O. Cutting edge: profile of chemokine receptor expression on human plasma cells accounts for their efficient recruitment to target tissues. *J Immunol*. 2003;170:1136-1140.
23. Sanz-Rodriguez F, Hidalgo A, Teixido J. Chemokine stromal cell-derived factor-1alpha modulates VLA-4 integrin-mediated multiple myeloma cell adhesion to CS-1/fibronectin and VCAM-1. *Blood*. 2001;97:346-351.
24. Parmo-Cabanas M, Bartolome RA, Wright N, Hidalgo A, Drager AM, Teixido J. Integrin alpha4beta1 involvement in stromal cell-derived factor-1alpha-promoted myeloma cell transendothelial migration and adhesion: role of cAMP and the actin cytoskeleton in adhesion. *Exp Cell Res*. 2004;294:571-580.
25. Parmo-Cabanas M, Molina-Ortiz I, Matias-Roman S, et al. Role of metalloproteinases MMP-9 and MT1-MMP in CXCL12-promoted myeloma cell invasion across basement membranes. *J Pathol*. 2006;208:108-118.
26. Grignani G, Perissinotto E, Cavalloni G, Carnevale Schianca F, Aglietta M. Clinical use of AMD3100 to mobilize CD34+ cells in patients affected by non-Hodgkin's lymphoma or multiple myeloma. *J Clin Oncol*. 2005;23:3871-3872; author reply 3872-3873.
27. Leleu X, Jia X, Runnels J, et al. The Akt pathway regulates survival and homing in Waldenstrom macroglobulinemia. *Blood*. 2007;110:4417-4426.
28. Shenker BJ HR, Zekavat A, Yamaguchi N, Lally ET, Demuth DR. Induction of apoptosis in human T cells by *Actinobacillus actinomycetemcomitans* cytolethal distending toxin is a consequence of G2 arrest of the cell cycle. *J Immunol*. 2001;167(1):435-41.
29. Sotillo R, Dubus P, Martin J, et al. Wide spectrum of tumors in knock-in mice carrying a Cdk4 protein insensitive to INK4 inhibitors. *EMBO J*. 2001;20:6637-6647.
30. Mitsiades CS, Mitsiades NS, Bronson RT, et al. Fluorescence imaging of multiple myeloma cells in a clinically relevant SCID/NOD in vivo model: biologic and clinical implications. *Cancer Res*. 2003;63:6689-6696.
31. Mitsiades CS, Mitsiades NS, McMullan CJ, et al. Inhibition of the insulin-like growth factor receptor-1 tyrosine kinase activity as a therapeutic strategy for multiple myeloma, other hematologic malignancies, and solid tumors. *Cancer Cell*. 2004;5:221-230.
32. Novak J, Georgakoudi I, Wei X, Prossin A, Lin CP. In vivo flow cytometer for real-time detection and quantification of circulating cells. *Opt Lett*. 2004;29:77-79.
33. Sipkins DA, Wei X, Wu JW, et al. In vivo imaging of specialized bone marrow endothelial microdomains for tumour engraftment. *Nature*. 2005;435:969-973.
34. Hideshima T, Chauhan D, Ishitsuka K, et al. Molecular characterization of PS-341 (bortezomib) resistance: implications for overcoming resistance using lysophosphatidic acid acyltransferase (LPAAT)-beta inhibitors. *Oncogene*. 2005;24:3121-3129.
35. Hideshima T, Bergsagel PL, Kuehl WM, Anderson KC. Advances in biology of multiple myeloma: clinical applications. *Blood*. 2004;104:607-618.
36. Anderson KC, Kyle RA, Dalton WS, et al. Multiple Myeloma: new insights and therapeutic approaches. *Hematology Am Soc Hematol Educ Program*. 2000:147-165.
37. Hideshima T, Mitsiades C, Akiyama M, et al. Molecular mechanisms mediating antimyeloma activity of proteasome inhibitor PS-341. *Blood*. 2003;101:1530-1534.
38. Liles WC, Rodger E, Broxmeyer HE, et al. Augmented mobilization and collection of CD34+ hematopoietic cells from normal human volunteers stimulated with granulocyte-colony-stimulating factor by single-dose administration of AMD3100, a CXCR4 antagonist. *Transfusion*. 2005;45:295-300.
39. Devine SM, Flomenberg N, Vesole DH, et al. Rapid mobilization of CD34+ cells following administration of the CXCR4 antagonist AMD3100 to patients with multiple myeloma and non-Hodgkin's lymphoma. *J Clin Oncol*. 2004;22:1095-1102.
40. Flomenberg N, Devine SM, Dipersio JF, et al. The use of AMD3100 plus G-CSF for autologous hematopoietic progenitor cell mobilization is superior to G-CSF alone. *Blood*. 2005;106:1867-1874.